SHAFT SIZING FOR MULTISTAGE PUMPS

by

Ulrich Bolleter

Director of Technology, Pump Division

and

Arno Frei

Head, Mechanical Development Group

Sulzer Brothers Limited

Winterthur, Switzerland

Ulrich Bolleter graduated from Winterthur Technical College (1966), Switzerland, with a degree in Electrical Engineering, holds an M.S. degree from Arizona State University (Mechanical Engineering), and a Ph.D. degree (Engineering) from Purdue University. He is Director of Technology of the Pump Division of Sulzer Brothers Limited, Winterthur, Switzerland. He joined Sulzer as a Research Engineer in the Laboratory for Vibrations and Acoustics (1971). In 1978, he became the manager of this laboratory and was involved in most of Sulzer's products in the areas of noise control, dynamics and vibrations, including extensive experience with pumps.

Arno Frei graduated (1959) from St. Gall Technical College, Switzerland, with a degree in Mechanical Engineering. He joined Sulzer in 1966 and was first engaged in the design and development of primary recirculation pumps for nuclear power stations. After activities in the field of nuclear heat exchangers, he rejoined the pump division, where he has been Head of the Mechanical Development Group since 1978.

ABSTRACT

For proper sizing of pump shafts, many criteria need be considered such as stress, deformation, and rotordynamics. The authors try to shed more light on these areas in order to ensure economic, safe, and reliable pump operation.

INTRODUCTION

Undoubtedly, a properly designed shaft is one of the key success factors for high reliability of pumps. Often, the feeling is "The thicker the shaft, the better," and pumps are praised (or cursed), based on shaft thickness. Reference is made to "stiff shaft designs," often without definition of this term. Concerning hydraulic behavior, it is undisputed that thinner shafts tend to increase efficiency, head coefficient, and improve suction behavior. The purpose herein is to shed more light on these conflicting requirements, to clarify terminologies, and to review shaft sizing procedures with respect to stresses, deflection and rotordynamic behavior. A simplified model is used for ease and consistency of parameter studies. The study applies to multistage pump rotors as typically shown in Figure 1, with three and more stages. The two rotors shown in Figure 1 serve as examples for the arguments presented. The relevant data are shown in Table 1. Machines with back-to-back impeller arrangements are not directly modelled, but most of the conclusions also apply.

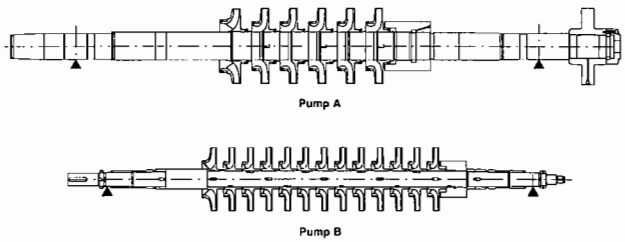

Figure 1. Rotors of Sample Pumps (to Same Scale).

Table 1. Data of Sample Pumps.

Line		Pump A	Pump B
1	Pump Type	HPT	GSG
2	Speed (RPM)	6260	3550
3	Head H_{tot} (m/ft)	3028/9934	1716/5630
4	Flow (l/s, GPM)	226.4/3590	45/714
5	Rotor mass (kg/lb)	491/1083	168/370
6	Stages	6	13
7	Shaft diameter, D_w (mm/in)	118.6/4.67	70/2.76
8	Bearing span, L (mm/in)	1998/78.7	1951/76.8
9	Impeller dia, D_2 (mm/in)	320/12.60	270/10.63
10	Specific speed n_q (m,m^3/s//ft,GPM)	26/1482	19/1083
11	Dia. clearances, $2h_o$, new (mm/in)	.45/.0177	.5/.0197

There are two basic types of rotor design, "individual impeller fixation" (Pump A) and "integral impeller fixation" (Pump B). The latter is well proven for pumps with a head per stage not exceeding about 200 m (650 ft), and a total head not over about 2000 m, these limits being dependent on the design, materials, type of liquid, and severity of temperature transients. Where applicable, this design is economical both in initial cost and for maintenance. For higher requirements, individual impeller fixation is chosen, with impellers individually shrunk on and axially secured. Just as important as overall shaft sizing is a careful design. Threads must be avoided in highly stressed areas, and grooves need be carefully designed to minimize stress concentrations. To avoid fretting corrosion, and for ease of maintenance, major components such as coupling,

balance drum, and thrust collar may be fixed by hydraulic shrink fits, as shown in Figure 1 for pump A.

In designing a shaft, both stress levels and deflections under static and dynamic loads need be considered. Concerning deflection, sometimes the ratio L^3/D_w^4 is used for judging shaft stiffness. It is a factor proportional to the deflection of a beam under a static load. This ratio should not be used for judging multistage pumps, as the load is not related to the pump, nor is the deflection related to the clearances, that is, the criterion is completely independent of pump size, speed etc. Furthermore, dynamic behavior is disregarded altogether. Another attempt in providing simple guidelines is the guidance chart shown in Figure 2 [1]. Although attractive on first sight, it has serious shortcomings. From simple beam theory it can be deduced that the design lines represent constant ratios of natural frequency in air to rotational frequency. The "Recommended Design Line" corresponds to a ratio of approximately 0.3; for pumps with dry running capability, the ratio is approximately 0.55. While the latter makes sense for the dry running condition, there is no explicit consideration for the wet running condition, and, as will be seen later, there is no reason for a pump with a natural frequency ratio in air of 0.3 to be better than a pump with a different frequency ratio. These considerations also illustrate that taking the various parameters and conditions into account is no simple matter, and that it is virtually impossible to give a simple criterion.

SIZING OF SHAFTS FOR STRESS

At the minimum, a shaft must be sized to safely transmit the maximum torque. Often, rough sizing of a shaft is based on a nominal torsional stress at the coupling, τ_0. Typical levels for τ_0 as a function of material yield strength are shown in Figure 3, together with the actual values of the two sample pumps. The safety factor against yield using Mises' criterion is calculated as:

$$S = \frac{\sigma y}{\sqrt{3}\cdot\tau_0} \quad => \quad \tau_0 = \frac{\sigma y}{S\cdot\sqrt{3}} \qquad (1)$$

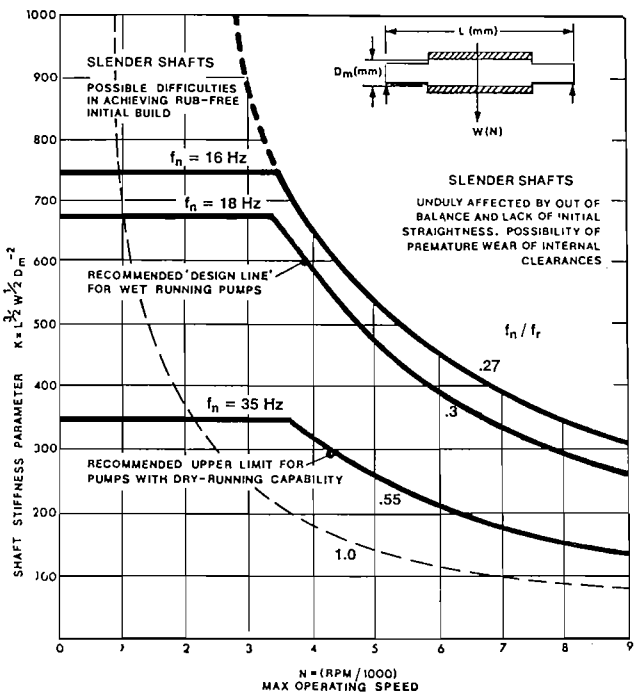

Figure 2. Guidance Chart for Shaft Diameter of between Bearing Rotors [1]. Dashed line and frequency indications by authors.

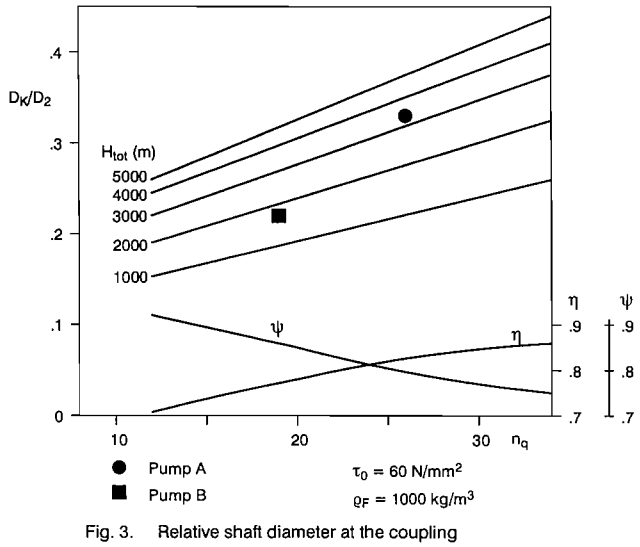

Fig. 3. Relative shaft diameter at the coupling

Figure 3. Typical Nominal Torsional Stress Level at the Coupling as a Function of Yield Strength.

For high strength shaft materials, τ_0 has to be limited mainly for reasons of safe torque transfer via keys or shrinkfits from the coupling hub to the shaft and back onto the impellers.

Given the allowable nominal torsional stress, the necessary shaft diameter at the coupling can be calculated from basic pump data [2]:

$$\frac{D_k}{D_2} = \sqrt[3]{\frac{\rho_F H_{tot}\cdot\psi^{3/2} n_q^2}{1268\,\eta\cdot\tau_0}} \qquad (2)$$

This relationship is shown in Figure 4 for a τ_0 of 60 N/mm2, again with the actual values of the two sample pumps. An approximate relationship for the efficiency and the head coefficient was assumed as indicated in Figure 4.

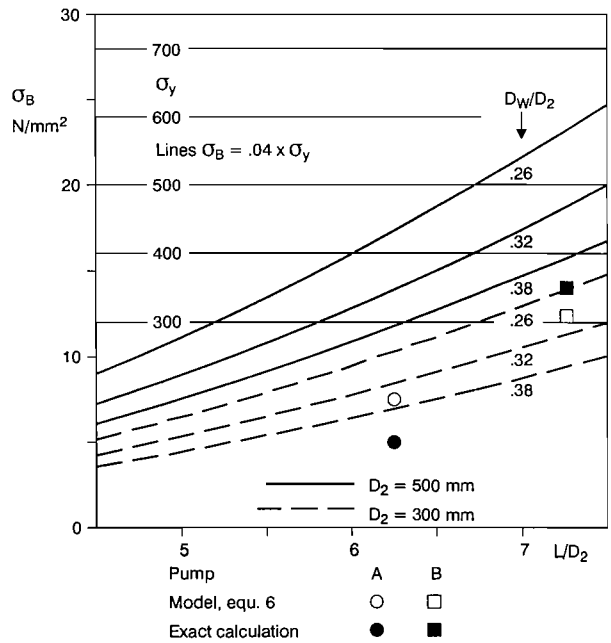

Figure 4. Relative Shaft Diameter at the Coupling.

Of course, the selected torsional stress has to reflect many viewpoints such as design details (stress raisers), influence of the liquid pumped, and its operating temperature on material properties like yield strength and, particularly, the endurance limit.

A shaft with sizing according to Figure 3 is normally safe against transient moments of the driver, notably peak moments of electrical motors during startups, or electrical faults, such as fast reclosure or shorts, see Dittrich for example [3]. Typically, for an asynchronous motor, peak torque in the air gap is 10 times the nominal torque. The short term transient excitation contains once and twice line frequency components. The peak torque arriving at the coupling of a motor pump system can be estimated as:

$$M_k = M_{air} \frac{I_P}{I_P+I_M} \cdot RS \qquad (3)$$

The response spectrum RS is the normalized peak torque at the coupling as a function of the system torsional natural frequency. For a simple motor-coupling-pump system, typical values are:

$$\frac{M_{air}}{M_0} \leq 10 \qquad (4)$$

$$\frac{I_P}{I_P+I_M} \leq 0.1$$

$$RS \leq 2, \text{ if } f_n/f_L \text{ and } f_n/2f_L \leq 0.7$$

From Equation 3 and 4 the ratio of the maximum torque at the coupling to the nominal torque is:

$$\frac{M_k}{M_0} \leq 10 \cdot 0.1 \cdot 2 = 2 \qquad (5)$$

Thus, if the conditions of Equation (4) are fulfilled, and a safety factor ≥4 against yield is maintained, the rotor is safe against yield during typical motor transients. If the limits of Equation (4) are exceeded, or if the system is more complex, then a detailed transient torsional analysis must be carried out, Frei, et al. [4].

A rough check can also be made on the dynamic bending stress against the fatigue limit. Dynamic bending stress is generated by rotation of the shaft in its statically deformed position, or in any other static bending line such as one forced by the action of labyrinths. As will be seen later, for properly designed pumps and proper rotor settings, the dynamic bending stress does not normally exceed the static stress under gravity loading. This can be estimated from simple beam theory. Assuming all the components attached to the rotor to be concentrated at mid span:

$$\sigma_B = \frac{L^2}{D_2} \frac{\left[1+2\frac{W_c}{W_s}\right]}{D_w/D_2} \rho_R \cdot g \qquad (6)$$

For a typical value of $W_c/W_s = 1$, resulting stress levels are shown in Figure 5. The larger the machine, with otherwise the same proportions, the larger is the stress level. Results from the sample pumps indicate adequate accuracy of the simple beam model. Assuming a fatigue limit of 0.25 σ_y, a safety factor of 2.0, and a combined stress concentration and notch sensitivity factor of 3.0, the nominal bending stress should not exceed 0.04 σ_y. These limits are indicated in Figure 5 for various yield stresses and can be used as a guide for the need for a more detailed analysis. If the preceding conditions apply, and if the material has a yield strength of at least 500 N/mm² (71,000 psi), then the dynamic bending stress due to the static rotor bending line is not a problem, unless the pump is large (impeller diameter above 500 mm (20 in)) and has many stages, leading to a relative bearing span L/D_2 of more than 7.

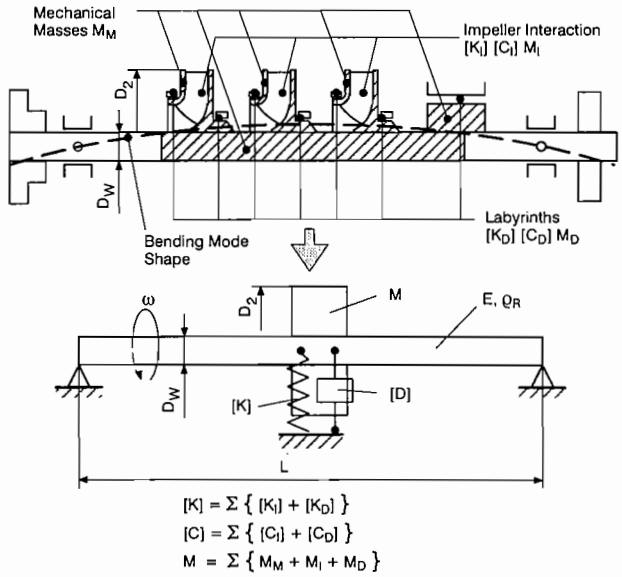

Figure 5. Nominal Bending Stress Due to Static Deformation.

The preliminary shaft sizing presented so far does not relieve the designer from requiring a detailed stress analysis of the entire rotor for new designs, new applications, or unusual loading conditions. Typically such an analysis would include static loads due to the drive torque and axial thrust, *as well as* dynamic loads, due to alternating torque and shaft bending. Stress concentration and notch sensitivity factors also need to be included. Combined static and dynamic stress levels are calculated and compared to required safety factors on fatigue and yield.

Having sized a rotor for stress, the question arises whether it should be made thicker for reasons of deflections or rotordynamics. This will be investigated in the next sections.

A SIMPLIFIED ROTOR MODEL

For the analysis of a wide range of geometrical and operational parameters, it is convenient to use a simplified rotor model. This is based on a "Jeffcott" or "Laval" rotor model, that is, on a simply supported beam with all masses and forces concentrated at midspan. The modelling process is shown in Figure 6. Geometries, masses, interaction coefficients, and the effect of the piston were chosen to match reasonably well actual pumps of the types shown in Figure 1. Labyrinth coefficients are based on Florjancic, et al. [5], impeller interaction coefficients in Bolleter, et al. [6]. Main data for the model are contained in Table 2. A particular problem in modelling is the relationship of the normalized shaft length L/D_2 to the number of stages. The dilemma is indicated in Figure 7. Depending on specific speed and design, the number of stages for a given rotor length and impeller diameter varies strongly. For the model, an average was chosen as indicated also in Figure 7. Except for pumps with three or possibly four stages, the results are not very sensitive to a wrong number of stages. This is supported by the quite reasonable fits of the two sample pump calculations. From the simple model, quantities of interest, such as static bending, natural frequency in air and under operation, damping,

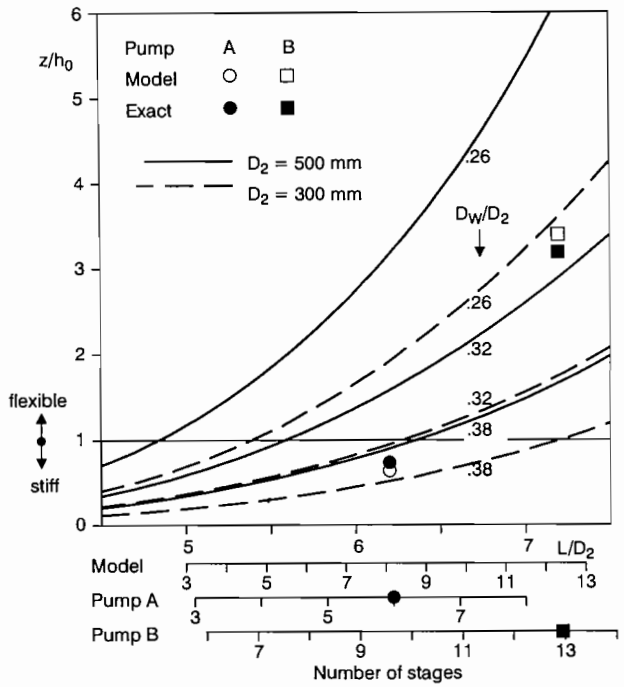

Figure 6. Simplified Model of a Multistage Rotor.

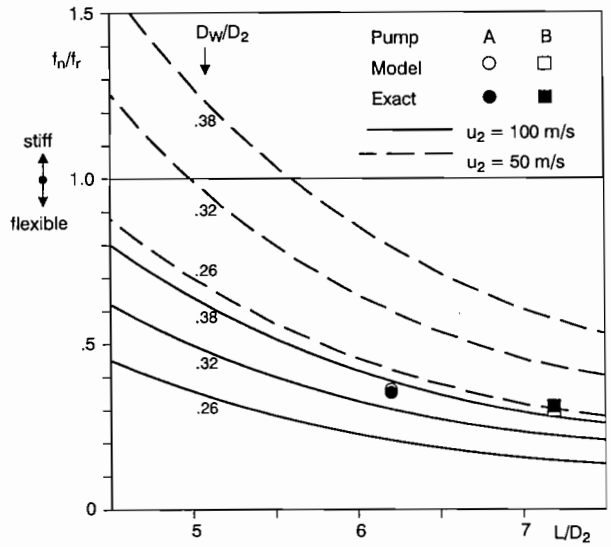

Figure 7. Relative Static Deflection, No Rotation.

response to static and dynamic forces, and the effect of an initial rotor bow, can now be calculated easily for different shaft thicknesses, bearing spans, circumferential speeds, labyrinth clearances, fluid densities, etc.

This model has limitations one should be aware of. First, the effect of the bearings is not included. For short shafts (and with low stage numbers) natural frequencies may be lowered, and damping increased compared to results from the model. Indeed for such pumps, calculated damping values are generally higher than indicated by the model. To compensate for this to some extent, damping was increased in the model by setting the coefficient k_s = 0.34 for short pumps, as indicated in Table 2. For longer pumps the effect of bearings on the classical first bending mode of pumps is quite negligible as can be seen from the good correspondence

Table 2. Data for the Model. (1) for $L/D_2 \le 5$ (≤ 3 stages): $k_{c*} = 0.34$ with swirl brake: reduce by factor two; Clearances, $2h_0$, new: $0.0017 \cdot D_2$, worn: $.0034 \cdot D_2$; Speed of sound c_s (m/s): 5100; Spec. gravity of rotor material: 7.85; Spec. gravity of liquid: 1.00 and 0.50; Relative impeller width B_2/D_2: 0.1; Head coefficient ψ: 1.

	k^*	k_c^*	c^*	c_c^*	m^*	Definition
Labyrinths	0,4	0,4 (1)	0,43	0	0,1	$k^*, k_c^* = \frac{h}{L_D \cdot R_D \cdot \Delta p_D} \cdot (k, k_c)$ $c^*, c_c^* = \frac{h\,\omega}{L_D \cdot R_D \cdot \Delta p_D} \cdot (c, c_c)$ $m^* = \frac{h\,\omega^2}{L_D \cdot R_D \cdot \Delta p_D} \cdot m$
Impeller Interaction	−2.5	7,5	3,5	7,5	8,5	$k^*, k_c^* = \frac{1}{\pi \cdot R_2^2 B_2 \cdot \varrho_F \cdot \omega^2} \cdot (k, k_c)$ $c^*, c_c^* = \frac{1}{\pi \cdot R_2^2 B_2 \cdot \varrho_F \cdot \omega} \cdot (c, c_c)$ $m^* = \frac{1}{\pi \cdot R_2^2 B_2 \cdot \varrho_F} \cdot m$

(1) for $L/D_2 \le 5$ (≤ 3 stages) : $k_c^* = .34$
with swirl brake: reduce by factor two

Clearances, $2h_0$, new: $.0017 \cdot D_2$, worn: $.0034 \cdot D_2$
Speed of sound c_s (m/s): 5100
Spec. gravity of rotor material: 7.85
Spec. gravity of liquid: 1.00 and .50
Relative impeller width B_2/D_2: .1
Head coefficient Ψ: 1

between model results and results from exact calculations on the sample pumps. A further limitation of the model is that it does not include the shaft overhangs, notably the drive end shaft overhang with the coupling. Coupling dominated critical speeds are not modelled and therefore not included in the analysis. Some remarks concerning this are included in the last section.

STIFF AND FLEXIBLE ROTORS

As mentioned in the INTRODUCTION, there is uncertainty concerning the meaning of the terms "stiff" and "flexible" rotors. This largely stems from the fact that pumps behave so differently in air and under operation in liquid. For clearness of definition, it is proposed here to use either a static criterion or a dynamic one based on the rotor behavior in air. For the first criterion, the static sag is compared to the radial labyrinth clearances. The ratio is given by:

$$\frac{z}{h_0} = \phi^2 \frac{gD_2}{c_s^2} \left[\frac{D_2}{D_W}\right]^4 \left[\frac{L}{D_2}\right]^3 \frac{D_2}{h_0} \qquad (7)$$

$$\phi = \left[\frac{4}{3\pi} \cdot \frac{M}{\rho_R \cdot D_2^3}\right]^{1/2}$$

The result of a parameter study is shown in Figure 7. Included are values for the sample pumps calculated by the model and by an exact analysis. As expected, relative bearing span and shaft diameter play a major role. Also, the absolute size of the pump (impeller diameter) is important, with larger pumps being statically "softer." A static stiffness criterion can now be defined. A pump may be considered statically stiff if z/h0 is smaller than 1, that is, the static sag is smaller than the radial clearance. From Figure 7, it is obvious that only relatively small pumps with small relative bearing spans and relatively thick rotors could be considered statically stiff.

For the dynamic criterion, consider the natural frequency in air divided by the rotational speed frequency. This ratio is given by:

$$\frac{f_n}{f_r} = \frac{1}{2\,\phi\,(u_2/c_s)} \left[\frac{D_W}{D_2}\right]^2 \left[\frac{D_2}{L}\right]^{3/2} \qquad (8)$$

If the ratio is larger than 1, the rotor is considered dynamically stiff, as its natural frequency in air is higher than the rotational speed frequency, otherwise it is dynamically flexible, as indicated in Figure 8. Now this ratio depends, besides the geometrical parameters, on the circumferential speed. Clearly, only very short pumps with thick shafts and low circumferential speeds could be called dynamically stiff.

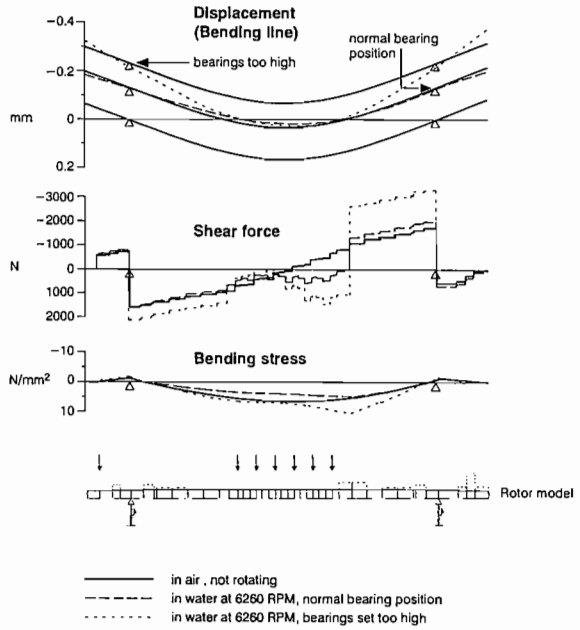

Figure 8. Natural Frequency in Air.

By these criteria then, most pumps would have to be considered statically and dynamically flexible. Unfortunately, there is no simple and unique definition which could be applied to pumps in operation in liquid. As will be seen, dynamic behavior is greatly changed. Static sag depends on rotor setting, design features, and operational parameters. Natural frequency and damping also depend on detailed design features, along with operating parameters, and (with high damping) the natural frequency to speed frequency ratio is of little significance. For all those reasons, one should stay away of trying to define a shaft stiffness criterion based on operation in liquid.

STATIC BENDING LINE AND ROTOR SETTING

As discussed before, the static bending line gives rise to dynamic bending stress under operation. Under the action of the labyrinth forces the static bending line, due to gravity, and with it the alternating bending stress, is changed. It is good practice to investigate this effect in order to avoid excessive alternating bending stress levels. The analysis is carried out with the help of a computer code taking into account iteratively the nonlinear bearing coefficients, the supporting effect of the labyrinths and the impellers, and the bending stiffness of the rotor. The results are the static bending line, bending stress and shear force along the rotor. Such an analysis is illustrated in Figures 9 and 10 for the two sample pumps.

Pump A, which would classify as a statically stiff pump, is shown in Figure 9. The sag of 0.16 mm (6.3 mil) is compensated in this design by lifting the bearings by 0.135 mm (5.3 mil). This brings the impellers and the piston about into the center for the nonrotating pump, and ensures adequate bearing loading under operation, as can be seen from the shear force diagram. The

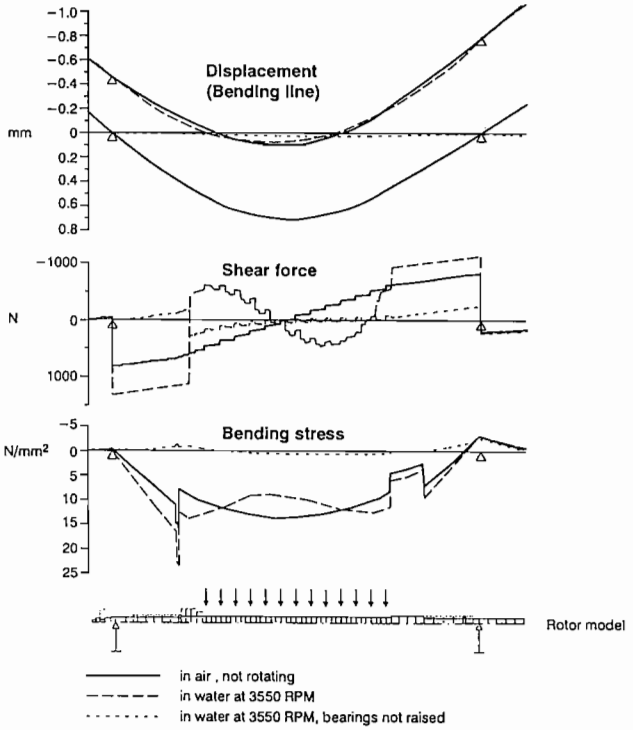

Figure 9. Static Shaft Displacement, Shear Force and Bending Stress of Pump A.

bending stress stays about the same as in air. Rotor setting for this relatively stiff machine is, however, quite sensitive. Increasing the bearing offset by only 0.1 mm (4 mil) more than doubles the bending stress.

Pump B, shown in Figure 10, is a statically soft machine, with the static sag being about three times the clearances. Thus, this pump would rub on startup if no measures were taken. As shown in Figure 10, it would center itself very nicely in operation under the forces of the labyrinths, and bending stresses would be very low. However, in this case, bearing load would be too low, and heavy rubs on startup and stopping are normally not desirable. Therefore, the bearings again are set higher, in this case by 0.4 mm (1.57 mil) on the outboard side and 0.8 mm (3.15 mil) on the inboard side. This is accomplished by tilting the bearing housings slightly up. There is now no rub on startup, and bending stress and bearing load are similar to the condition in air, that is, quite acceptable. There are other methods to ensure rub free initial build such as tilting certain stage casings or "sag boring" a horizontally split pump. All these methods need careful analysis of the bending line and the ensuing bending stresses and bearing loads under operation, as well as careful machining, assembly and maintenance.

EFFECT OF SHAFT THICKNESS ON NATURAL FREQUENCY AND DAMPING

Based on the model, natural frequencies and damping values were calculated for a wide range of parameters, as shown in Figures 11 and 12. The large effect of the liquid is immediately apparent on comparison with Figure 8. In most cases, the natural frequency is above the operating speed frequency. For high circumferential speed, the natural frequency ratio even increases with increasing relative bearing span, that is with the number of stages, contrary to the situation in air. Rotor thickness has a significant effect only at the lower circumferential speed and for low relative

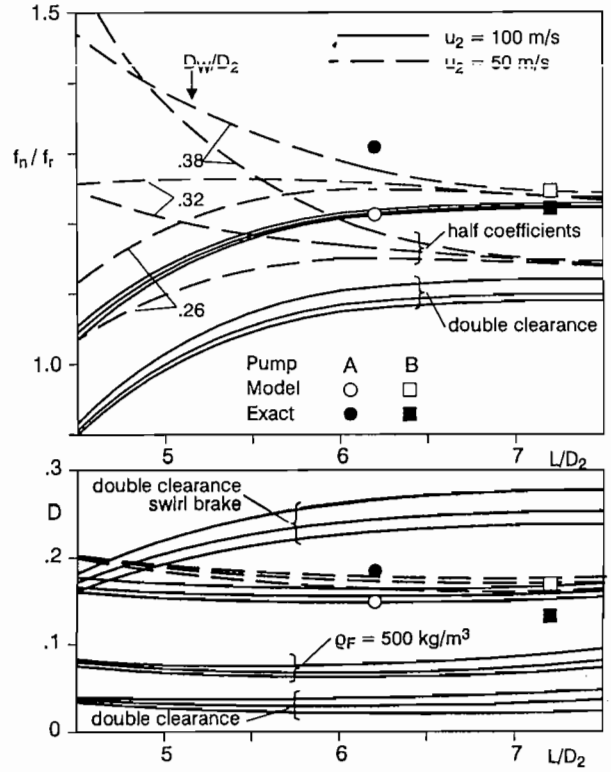

Figure 10. Static Shaft Displacement, Shear Force and Bending Stress of Pump B.

rotor length. In all other cases, and particularly also concerning damping, rotor thickness has no influence. Even when the interaction coefficients are reduced to half, shaft thickness has a significant influence only for low circumferential speed and for pumps with a relative bearing span below about 5.5, that is, for pumps with five or less stages. It is clear from this analysis that stiffness forces in the labyrinths dominate rotor stiffness forces. With worn clearances, the natural frequency drops close to the rotational

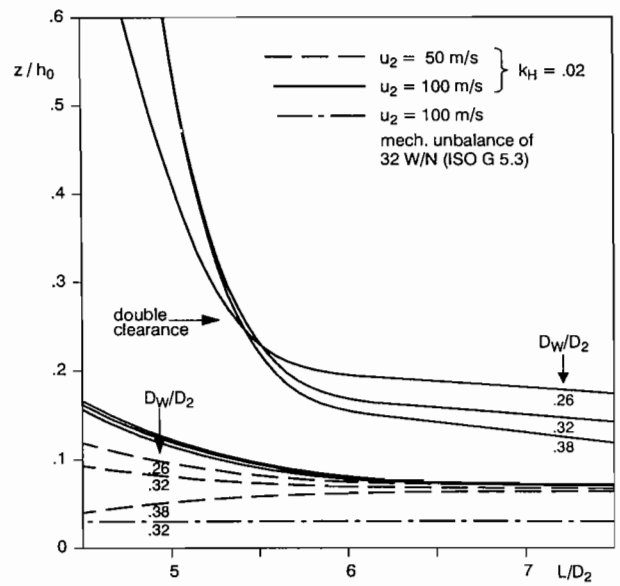

Figure 11. Natural Frequency Ratio and Damping Factor in Operation in Liquid (u_2 = 50 m/s).

speed frequency and the damping decreases drastically. A similar effect has the reduction of the density of the fluid. The use of swirl breaks [7] dramatically increases damping and would allow these pumps to be safely operated at worn clearances.

Indeed the two sample pumps fitted with swirl breaks at the piston show very good behavior at worn clearances. This figure does indicate that for pumps with more than about five stages the natural frequency and damping is almost entirely determined by the interaction forces in the labyrinths, the impellers and the piston. Thus, the pump is quite sensitive to design features in these areas, particularly at increased clearances. Research in these areas has been and continues to be very active [8, 9, 10].

EFFECT OF SHAFT THICKNESS ON THE DEFLECTION UNDER EXCITATION FORCES

Most obvious are forces at the rotational speed frequency such as mechanical and hydraulic unbalance. The relative shaft displacement is shown in Figure 13 under such forces for new and worn labyrinths. Mechanical unbalance was assumed to be 8 times the limit of API 610 7th edition [11], which corresponds to an unbalance of about G 5.3 according to ISO 1940 [12]. With this unbalance, the rotor deflection is less than five percent of the clearances, thus quite insignificant. Of more importance is the hydraulic unbalance, a force generated by small deviations from the ideal impeller geometry. It was found from experiments [6, 13], that a hydraulic force factor of $K_H = 0.02$ is not unusual even for precise impellers made by the lost wax casting process. The hydraulic unbalance force is given by:

$$F_H = K_H \cdot \rho_F \cdot \frac{B_2}{D_2} \cdot \frac{\psi}{2} \sqrt{n_{st}} \cdot u_2^2 \cdot D_2^2 \qquad (9)$$

It is essentially proportional to the circumferential speed squared, and to the machine size squared. As it is assumed that the phases of the hydraulic unbalance vectors of the impellers are random, thus compensating each other to some degree, the combined force

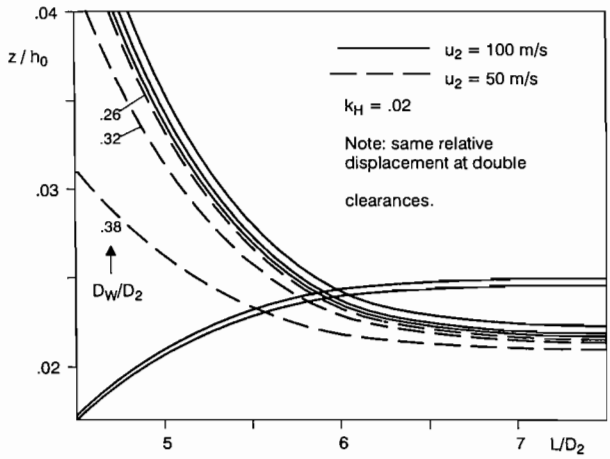

Figure 12. Natural Frequency Ratio and Damping Factor in Operation in Liquid (u_2 = 100 m/s).

is proportional to the square root of the number of stages. For new clearances, the shaft displacement remains below 20 percent of the clearances as shown in Figure 13, with insignificant dependance on shaft thickness. For double clearances and high circumferential speed the situation is more complex. As shown in Figure 12, there is a critical speed condition at about $L/D_2 = 5.0$ with relatively low damping. This leads to a high response to synchronous excitation,

notably hydraulic unbalance. Shaft displacement reaches on the order of 50 percent of the clearances, a situation which is unacceptable. Outside of the resonance area, shaft displacement again remains below 20 percent of clearances. Removing the critical speed is hardly possible, as the shaft thickness has little influence (Figure 12). The best remedy is to increase damping by applying swirl brakes, at least at the piston. Shaft displacement is then brought back to levels similar to the case with new clearances.

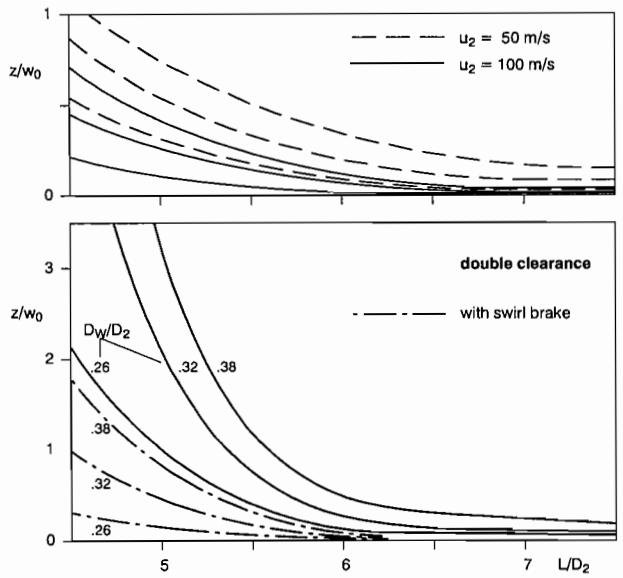

Figure 13. Relative Shaft Displacement Due to Hydraulic and Mechanical Unbalance.

Next, shaft displacement to static radial thrust is considered. Such forces again are created by geometrical deviations, particularly of the stationary components such as diffusers or volutes. Even though these are rotationally symmetric (single volutes not being considered here) hydraulic radial force coefficients were experimentally determined to be in the range of 0.01 to 0.06, depending on relative flow and geometrical accuracy [6, 13]. Calculations shown in Figure 14 were done with K_H = 0.02. The resulting radial displacements are generally less than five percent

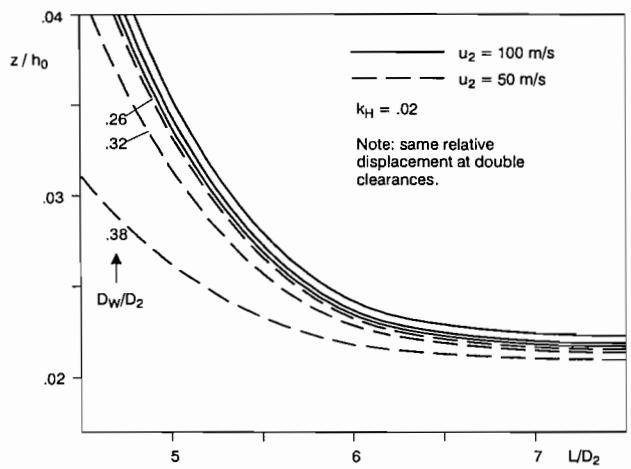

Figure 14. Relative Shaft Displacement Due to Static Radial Hydraulic Thrust. (Similar for low frequency dynamic hydraulic thrust).

of the clearances in new and worn conditions. Again, shaft thickness plays a certain role only for short pumps and low circumferential speeds.

The results of Figure 14 are also approximately applicable to low frequency hydraulic excitation forces as encountered at low part load flows. Hydraulic force coefficients may reach values of 0.15 at those conditions [6, 13] which could bring shaft displacements to about 40 percent of clearances for pumps with a low number of stages and high circumferential speeds. Again, increasing the shaft thickness does not change much as the forces in the labyrinths dominate. These conclusions do not apply, of course, to single or possibly two stage pumps, as with those the shaft stiffness usually dominates. Shafts for high head, single stage, double suction pumps, such as nuclear feed pumps or large pipeline pumps, must often be thicker than required by torque transmitted to limit deflections under static and low frequency hydraulic forces.

Another important excitation at rotational speed frequency is due to initial shaft bow. An initial shaft bow, always present in a pump rotor to some degree, not only creates a mechanical unbalance, but also interaction forces in the labyrinths due to the runout of the rotor. These interaction forces tend to straighten the rotor in operation, while the unbalance forces tend to bend the rotor. The net effect, related to the initial shaft bow, is defined here as "amplification factor", z/w_0. If it is 1, then the shaft rotates under operation with an amplitude equivalent to the initial shaft bow. Note that balancing an assembled rotor in effect compensates the unbalance due to initial shaft bow, but does not remove the interaction forces. If, under operation, the shaft is straightened, at least to some extent, the correction weights act as unbalances [14]. Rather than balancing an assembled rotor, it should be checked for acceptable runout and acceptable state of balance only. Should these not be acceptable, the rotor should be disassembled and the out of balance components be corrected. Shaft bow amplification factors are shown in Figure 15 to be generally below 1.0 for new clearances. The thicker the shaft, the higher is the amplification factor. As generally admissible, shaft initial bow (shaft runout) is

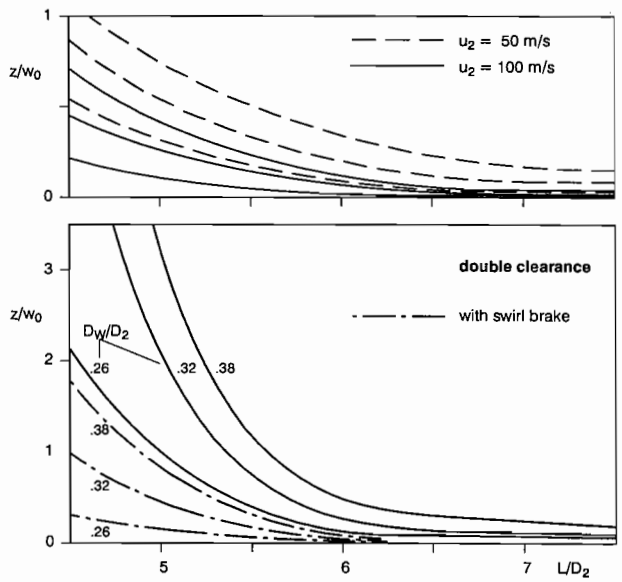

Figure 15. Shaft Bow Amplification Factor.

considerably smaller than the clearances. Its effect is of little consequence for new clearances. If, at increased clearances, a resonance condition is present, as is the case for high circumferen-

tial speed and L/D_2 about 5.0, the shaft amplification factor may increase strongly, in the model to values of about 3.0. Increasing the shaft thickness would only make the situation worse, while increasing the damping by swirl brakes reduces the amplification considerably.

CONCLUSIONS

As shown, pump shafts must primarily be sized for adequate stress levels. The shaft thickness needed at the coupling can be estimated from an acceptable nominal torsional stress and from global pump operating parameters, Equation (2), Figure 4. For new designs or applications, or for unusual loading conditions, a detailed stress analysis of the rotor is required, taking into account the static and dynamic loads, as well as notch effects on the rotor. For highly loaded rotors, threads and other high stress concentrations must be avoided. Whether a shaft must be made thicker than needed from a stress point can not simply be answered. Certainly criteria simply based on some shaft stiffness factors such as L^3/D_w^4 are inadequate, as are criteria based on the natural frequency in air.

Concerning the need to increase shaft thickness beyond values determined for stress levels, the most important conclusions are summarized in Table 3. Making the shaft thicker will generally not improve the dynamic behavior and the reliability of the pump, but would, of course, tend to degrade the hydraulic performance. Only pumps with low circumferential speed, below about 50 m/s (head per stage of about 150 m (500 ft)), and a low number of stages (three to five) would profit from shafts thicker than needed for stress reasons. In these cases, the mechanical rotor stiffness forces dominate the labyrinth and impeller interaction forces, and increasing the shaft thickness decreases the sensitivity to excitations. For higher circumferential speeds and higher stage numbers, the labyrinth and impeller interaction forces dominate the mechanical shaft stiffness forces. Rotordynamic reliability rests entirely on properly designed labyrinths. They must be sufficiently long, have shallow serrations or possibly no serrations, and, if resonance conditions are encountered at worn clearances, damping must be maintained high by swirl brakes or other means to reduce the swirl in the labyrinths, including the balance drum.

Table 3. Influence of Shaft Diameter. ↑ Advantage for increased shaft diameter. ↓ Disadvantage for increased shaft diameter. ↗ Increased shaft diameter has marginal advantage. → Shaft diameter has no practical influence.

Criterion	Influence of Shaft diameter		Comments
	$L/D_2 \leq 5.5$ (3-5 stages)	> 5.5 (> 5 stages)	
Natural frequency (wet)			
u_2 = 50 m/s (164 ft/s)	↑	→	
u_2 = 100 m/s (328 ft/s)	→	→	
Damping			
Shaft deflection due to			
- gravity (not rotating)	↗	↗	Rubfree build requires specia measures
- unbalance (hydraulic or mechan.)			For
u_2 = 50 m/s (164 ft/s)		→	worn clearances
u_2 = 100 m/s (328 ft/s	→	→	high damping required
- initial shaft bow			For
u_2 50 m/s	↓	→	worn clearances
u_2 = 100 m/s	↓	→	high damping required
- static thrust or low frequency radial forces			
u_2 = 50 m/s (164 ft/s)	↗	→	
u_2 = 100 m/s (328 ft/s)	→	→	
Alternating bending stress	↗	↗	

↑ Advantage for increased shaft diameter
↓ Disadvantage for increased shaft diameter
↗ Increased shaft diameter has marginal advantage
→ Shaft diameter has no practical influence

A reminder is necessary concerning the dynamic behavior of shaft overhangs, notably the coupling overhang. These have not been considered because the shaft was modelled between the bearings only. Good rotordynamic reliability can be reached only if the coupling end of the shaft has a low sensitivity to forces [15]. Rotor overhang, coupling, and bearing must be designed such that there is no critical speed encountered with a mode shape dominated by a deflection of the coupling overhang. Generally, a forced response analysis is necessary to ensure low sensitivity at the shaft coupling end, and criteria are given by Bolleter, et al. [15]. In this context, adequate static loading of the bearings is also important. Proper bearing offsets are needed, resulting from an analysis of the rotor bending line under the combined influence of bearing and labyrinth stiffnesses.

The results of the parameter study presented in the form of diagrams may serve to quickly judge whether a certain pump is in a region where shaft stiffness forces dominate or where labyrinth and impeller interaction forces dominate. Depending on this, increasing the shaft diameter may have a positive influence or not.

NOMENCLATURE

B_2	Impeller exit width
c	Damping coefficient
c_s	Speed of sound in rotor material
c_c	Crosscoupled damping coefficient
D	Damping factor (D=1 is critically damped)
D_k	Shaft diameter at the coupling
D_w	Shaft diameter at impellers
D_2	Impeller diameter
E	Modulus of elasticity of shaft
F_H	Hydraulic radial force
f_L	Line frequency
f_n	Natural frequency
f_r	Rotational speed frequency
g	Gravity
H_{tot}	Head of pump
h_0	Design clearance (radial) = "new" clearance
I_M	Moment of inertia of motor
I_P	Moment of inertia of pump
K_H	Hydraulic radial force coefficient
k	Stiffness coefficient
k_c	Crosscoupled stiffness coefficient
L	Bearing span
M	Mass at center of bearing span (Figure 6)
M_{air}	Torque in the air gap of the motor
M_k	Torque at the coupling
M_0	Motor nominal torque
m	Mass coefficient
n_q	Specific speed
n_{st}	Number of stages
RS	Normalized response spectrum of M_k due to motor transient
S	Safety factor as defined in Equation 1
u_2	Impeller circumferential speed
W_c	Weight of components on shaft
W_s	Weight of shaft alone
w_0	Initial shaft bow (1/2 TIR)
z	Rotor radial displacement
η	Efficiency

ρ_F Density of liquid
ρ_R Density of rotor material
σ_B Bending stress
σ_y Yield stress
τ_0 Nominal shaft stress at the coupling
ϕ Term defined in Equation (7)
ψ Head coefficient $= \dfrac{2 \cdot g \cdot H_{tot}}{u_2^2 \cdot n_{st}}$

REFERENCES

1. Duncan, A.B. and Hood, J.F., "The Application of Recent Pump Developments to the Needs of the Offshore Oil Industry," Conference on Pumps and Compressors for Offshore Oil and Gas, Aberdeen, I.Mech.E. Conf., Publ. 1976-8, paper C124/76, pp. 7-24 (1976).
2. Florjancic, D., Frei, A., and Simon, A., "Boiler Feed Pumps for Supercritical Power Plants—State of the Art," EPRI First International Conference on Coal-Fired Power Plants, Palo Alto, California (1986).
3. Dittrich O., "Drehmomentstösse beim Anfahren von Induktionsmotoren," (Torque surges when starting induction motors), Antriebstechnik *5* (9), pp. 317-322 (1966).
4. Frei, A., Luzi, A., Heil, W., and Grgic R., "Design of Pump Shaft Trains Having Variable Speed Electric Motors," *Proceedings of the Third International Pump Symposium*, Turbomachinery Laboratory, Department of Mechanical Engineering, Texas A&M University, College Station, Texas (1986).
5. Florjancic, S., Stuerchler, R., and McCloskey, T., "Annular Seals of High Energy Centrifugal Pumps: Presentation of Full Scale Measurement." 6th Workshop on Rotordynamic Instability Problems, Turbomachinery Laboratory, Department of Mechanical Engineering, Texas A&M University, College Station, Texas (1990).
6. Bolleter, U., Leibundgut E., Stuerchler, R., and McCloskey, T., "Hydraulic Interaction and Excitation Forces of High Head Pump Impellers," 3rd ASCE/ASME Mechanical Conference, San Diego, California, 1989, ASME Publication FED, *81* Pumping Machinery, pp. 187-193 (1989).
7. Valantas, R.A., and Bolleter, U., "Solutions to Abrasive Wear-Related Rotordynamic Instability Problems on Prudhoe Bay Injection Pumps," *Proceedings of the Fifth International Pump Users Symposium*, Turbomachinery Laboratory, Department of Mechanical Engineering, Texas A&M University, College Station, Texas (1988).
8. Childs, D.W., "Dynamic Analysis of Turbulent Annular Seals based on Hirs Lubrication Equation,", ASME Paper 82-Lub-41 (1982).
9. Childs, D.W., "Finite Length Solutions for Rotordynamic Coefficients of Turbulent Annular Seals," ASME Paper 82-Lub-42 (1982).
10. Nordmann, R., Dietzen, F.J., Janson, W., Frei, A., and Florjancic, S., "Rotordynamic Coefficients and Leakage Flow for Smooth and Grooved Seals in Turbopumps," IFTOMM Conference, Tokyo (1986).
11. "Centrifugal Pumps for General Refinery Service," API Standard 610, Seventh Edition (1989).
12. "Balance Quality of Rotating Rigid Bodies," International Standard ISO 1940, First Edition (1973).
13. Guelich, J.F., Jud, W., and Hughes, S.F., "Review of Parameters Influencing Hydraulic Forces on Centrifugal Impellers," Proceedings IMechE, *201* (A3), pp. 163-174 (1977).
14. Bolleter, U., and Frei, A., "Causes and Control of Synchronous Vibrations of Multistage Pumps," IMechE, London (1990).
15. Bolleter, U., Frei, A., and McCloskey, T., "How to Ensure Good Rotordynamic Behavior of High Energy Multistage Pumps," EPRI Power Plant Pumps Symposium, Tampa, Florida (1991).